

Joint Resource Partitioning and Offloading in Heterogeneous Cellular Networks

Sarabjot Singh and Jeffrey G. Andrews

Abstract—In heterogeneous cellular networks (HCNs), it is desirable to offload mobile users to small cells, which are typically significantly less congested than the macrocells. To achieve sufficient load balancing, the offloaded users often have much lower SINR than they would on the macrocell. This SINR degradation can be partially alleviated through interference avoidance, for example time or frequency resource partitioning, whereby the macrocell turns off in some fraction of such resources. Naturally, the optimal offloading strategy is tightly coupled with resource partitioning; the optimal amount of which in turn depends on how many users have been offloaded. In this paper, we propose a general and tractable framework for modeling and analyzing joint resource partitioning and offloading in a two-tier cellular network. With it, we are able to derive the downlink rate distribution over the entire network, and an optimal strategy for joint resource partitioning and offloading. We show that load balancing, by itself, is insufficient, and resource partitioning is required in conjunction with offloading to improve the rate of cell edge users in co-channel heterogeneous networks.

I. INTRODUCTION

The exponential growth in mobile traffic primarily driven by mobile video has led the drive to deploy low power base stations (BSs) both in licensed and unlicensed spectrum in order to complement the existing macro cellular architecture. Increased cell density increases the area spectral efficiency of the network [2] and is the key factor for the very large required capacity boost. Such a heterogeneous network (HetNet) consists of macro BSs coexisting with small cells formed by co-channel low power base stations like micro, pico and femto BSs, as well as unlicensed band WiFi access points (APs) [3], [4].

The “natural” association/coverage areas of the low power APs tend to be much smaller than those of the macro BSs, and hence the fraction of user population that is offloaded to small cells may often be limited, resulting in insufficient relief to the congested macro tier. This user load disparity not only leads to suboptimal rate distribution across the network, but the lightly loaded small cells may also lead to bursty interference causing QoS degradation [5], [6]. One practical technique for proactively offloading users to small cells is called cell range expansion (CRE) [3] wherein the users are offloaded through an association bias. A positive association bias implies that a user would be offloaded to a small cell as soon as the received power difference from the macro and small cell drops below

the bias value, which “artificially” expands the association areas of small cells¹. Though experiencing reduced congestion, in co-channel deployments such offloaded users also have degraded signal-to-interference-plus-noise-ratio (SINR), as the strongest AP (in terms of received power) now contributes to interference. Therefore, the gains from balancing load could be negated if suitable interference avoidance strategies are not adopted in conjunction with cell range expansion particularly in co-channel deployments [6]. One such strategy of interference avoidance is resource partitioning [3], [7], wherein the transmission of macro tier is periodically muted on certain fraction of radio resources (also called *almost blank subframes* in 3GPP LTE). The offloaded users can then be scheduled in these resources by the small cells leading to their protection from co-channel macro tier interference.

A. Motivation and Related Work

It has been established that without proactive offloading and resource partitioning only limited performance gains can be achieved from the deployment of small cells [8]–[12]. These techniques are strongly coupled and directly influence the rate of users, but the fundamentals of jointly optimizing offloading and resource partitioning are not well understood. For example, an excessively large association bias can cause the small cells to be overly congested with users of poor SINR, which requires excessive muting by the macro cell to improve the rate of offloaded users. Earlier simulation based studies [11], [12] confirmed this insight and showed that excessive biasing and resource partitioning can actually degrade the overall rate distribution, whereas the choice of optimal parameters can yield about 2-3x gain in the rate coverage (fraction of user population receiving rate greater than a threshold). Although encouraging, a general tractable framework for characterizing the optimal operating regions for resource partitioning and offloading is still an open problem. The work in this paper is aimed to bridge this gap.

A “straightforward” approach of finding the optimal strategy is to search over all possible user-AP associations and time/frequency allocations for each network configuration. Besides being computationally daunting, this approach is unlikely to lead to insight into the role of key parameters on system performance. Another methodology is a probabilistic analytical approach, where the network configuration is assumed random and following a certain distribution. This has the advantage of leading to insights on the impact of various system parameters

This work has been supported by the Intel-Cisco Video Aware Wireless Networks (VAWN) Program and NSF grant CIF-1016649. A part of this paper is accepted for presentation at IEEE Globecom 2013 in Atlanta, USA [1].

The authors are with Dept. of Electrical and Computer Engineering at the University of Texas, Austin (email: sarabjot@utexas.edu and jandrews@ece.utexas.edu).

¹Access point (AP), base station (BS), cell are used interchangeably in the paper.

on the average performance through tractable expressions. Analytical approaches for biasing and interference coordination were studied in [13]–[15], but downlink rate (one of the key metrics) was not investigated. Optimal bias and almost blank subframes were prescribed in [13] based on average per user spectral efficiency. A related SINR and mean throughput based analysis for resource partitioning was done in [14] and [16] respectively, but offloading was not captured. The choice of optimal range expansion biases in [15] was not based on rate distribution. In this paper, we use the metric of *rate coverage*, which captures the effect of both SINR and load distribution across the network. Semi-analytical approaches in [17], [18] showed, through simulations, that there exists an optimal association bias for fifth percentile and median rate which is confirmed in this paper through our analysis. Also, to the best of our knowledge, none of the mentioned earlier works considered the impact of backhaul capacities on offloading, which is another contribution of the presented work.

B. Approach and Contributions

We propose a general and tractable framework to analyze joint resource partitioning and offloading in a two-tier cellular network in Section II. The proposed modeling can be extended to a multiple tier setting as discussed in Sec. III-D. Each tier of base stations is modeled as an independent Poisson point process (PPP), where each tier differs in transmit power, path loss exponent, and deployment density. The mobile user locations are modeled as an independent PPP and user association is assumed to be based on biased received power. On all channels, i.i.d. Rayleigh fading is assumed. Similar tractable frameworks were used for deriving SINR distribution in HCNs in [19]–[21]. The empirical validation in [22] and theoretical validation in [23] for heavily shadowed cellular networks have strengthened the case of modeling macro cellular networks using a PPP. Due to the formation of random association/coverage areas in such network models, load distribution is difficult to characterize. An approximate load and rate distribution was derived for multiple radio access technology (RAT) HetNets in [24].

Based on our proposed approach, the contributions of the paper can be divided into two categories:

Analysis. The rate complementary cumulative distribution function (CCDF) in a two-tier co-channel heterogeneous network is derived as a function of the cell range expansion/offloading and resource partitioning parameters in Section III. Rate coverage at a particular rate threshold is the rate CCDF value at that threshold. The derived rate distribution is then modified to incorporate a network setting where APs are equipped with limited capacity backhaul. Under certain plausible scenarios, the derived expressions are in closed form. **Design Guidelines.** The theoretical results lead to joint resource partitioning and offloading insights for optimal SINR and rate coverage in Section IV. In particular, we show the following:

- With no resource partitioning, optimal association bias for rate coverage is independent of the density of the small cells. In contrast, offloading is shown to be strictly suboptimal for SINR in this case.

- With resource partitioning, optimal association bias decreases with increasing density of the small cells.
- In both of the above scenarios, the optimal fraction of users offloaded, however, increases with increasing density of small cells.
- With decrease in backhaul capacity/bandwidth the optimal association bias for the corresponding tier always decreases. However, in contrast to the trend in the “infinite”² backhaul scenario, the optimal association bias may increase with increasing small cell density.

The paper is concluded in Section V and future work is suggested.

II. DOWNLINK SYSTEM MODEL AND KEY METRICS

In this paper, the wireless network consists of a two-tier deployment of APs. The location of the APs of k^{th} tier ($k = 1, 2$) is modeled as a two-dimensional homogeneous PPP Φ_k of density (intensity) λ_k . Without any loss of generality, let the macro tier be tier 1 and the small cells constitute tier 2. The locations of users (denoted by \mathcal{U}) in the network are modeled as another independent homogeneous PPP Φ_u with density λ_u . Every AP of k^{th} tier transmits with the same transmit power P_k over bandwidth W . The downlink desired and interference signals from an AP of tier- k are assumed to experience path loss with a path loss exponent α_k . A user receives a power $P_k H_x x^{-\alpha_k}$ from an AP of k^{th} tier at a distance x , where H_x is the random channel power gain. The random channel gains are assumed to be Rayleigh distributed with average unit power, i.e., $H_x \sim \exp(1)$. General fading distributions can be considered at some loss of tractability [25]. The noise is assumed additive with power σ^2 . The notations used in this paper are summarized in Table I.

A. User Association

The analysis in this paper is done for a *typical* user u located at the origin. This is allowed by Slivnyak’s theorem [26], which states that the properties observed by a typical³ point of a PPP Φ is same as those observed by a node at origin in the process $\Phi \cup \{0\}$. Let Z_k denote the distance of the typical user from the nearest AP of k^{th} tier. It is assumed that each user uses biased received power association in which it associates to the nearest AP of tier j if

$$j = \arg \max_{k \in \{1, 2\}} P_k B_k Z_k^{-\alpha_k}, \quad (1)$$

where B_k is the association bias for k^{th} tier. Increasing association bias leads to the range expansion for the corresponding APs and therefore offloading of more users to the corresponding tier. For clarity, we define the *normalized* value of a parameter of a tier as its value divided by the value it takes for the serving tier. Thus,

$$\hat{P}_k \triangleq \frac{P_k}{P_j}, \quad \hat{B}_k \triangleq \frac{B_k}{B_j}, \quad \text{and} \quad \hat{\alpha}_k \triangleq \frac{\alpha_k}{\alpha_j},$$

²Infinite bandwidth implies sufficiently large so as not to affect the effective end-to-end rate.

³The term typical and random are interchangeably used in this paper.

TABLE I: Notation Summary

Notation	Description
$\Phi_k; \Phi_u$	PPP of APs of k^{th} tier; PPP of mobile users
$\lambda_k; \lambda_u$	Density of APs of k^{th} tier; density of mobile users
$P_k; \tilde{P}_k$	Transmit power of APs of k^{th} tier; normalized transmit power of APs of k^{th} tier
$B_k; \tilde{B}_k$	Association bias for k^{th} tier; normalized association bias for k^{th} tier.
$\alpha_k; \hat{\alpha}_k$	Path loss exponent of k^{th} tier; normalized path loss exponent of k^{th} tier
$W; O_k$	Air interface bandwidth at an AP for resource allocation; backhaul bandwidth at an AP of k^{th} tier
\mathcal{U}_l	Macro cell users $l = 1$, small cell users (non-range expanded) $l = \bar{B}$, offloaded users $l = B$
$\eta; \gamma_l$	Resource partitioning fraction; inverse of the effective fraction of resources available for users in \mathcal{U}_l
$J(l)$	Map from user set index to serving tier index, $J(1) = 1$, $J(\bar{B}) = J(B) = 2$
σ^2	Thermal noise power
\mathcal{A}_l	Association probability of a typical user to \mathcal{U}_l
$\mathcal{R}; \mathcal{S}; \rho$	Rate coverage; SINR coverage; rate threshold
$N_l; p_l(n)$	Load at tagged AP of $u \in \mathcal{U}_l$; PMF of load $p_l(n) = \mathbb{P}(N_l = n)$
$Z_k; Y_l$	Distance of the nearest AP in k^{th} tier; distance of the tagged AP conditioned on $u \in \mathcal{U}_l$
$\mathcal{C}_{x_k}; \mathcal{C}_k$	Association region; area of an AP of tier k

are respectively the normalized transmit power, association bias, and path loss exponent of tier k conditioned on the user being associated with tier j . In this paper, association bias for tier 1 (macro tier) is assumed to be unity ($B_1 = 0$ dB) and that of tier 2 is simply denoted by B , where $B \geq 0$ dB. In the given setup, a user $u \in \mathcal{U}$ can lie in the following three disjoint sets:

$$u \in \begin{cases} \mathcal{U}_1 & \text{if } j = 1, P_1 Z_1^{-\alpha_1} \geq P_2 B Z_2^{-\alpha_2} \\ \mathcal{U}_{\bar{B}} & \text{if } j = 2 \text{ and } P_2 Z_2^{-\alpha_2} > P_1 Z_1^{-\alpha_1} \\ \mathcal{U}_B & \text{if } j = 2 \text{ and } P_2 Z_2^{-\alpha_2} \leq P_1 Z_1^{-\alpha_1} < P_2 B Z_2^{-\alpha_2}, \end{cases} \quad (2)$$

where $\mathcal{U}_1 \cup \mathcal{U}_B \cup \mathcal{U}_{\bar{B}} = \mathcal{U}$ clearly. The set \mathcal{U}_1 is the set of macro cell users and the set $\mathcal{U}_{\bar{B}}$ is the set of unbiased small cell users. Thus, the set $\mathcal{U}_{\bar{B}}$ is independent of the association bias. The users offloaded from macro cells to small cells due to cell range expansion constitute \mathcal{U}_B and are referred to as the *range expanded users*. All the users associated with small cells are $\mathcal{U}_2 \triangleq \mathcal{U}_{\bar{B}} \cup \mathcal{U}_B$. We define a mapping $J : \{1, \bar{B}, B\} \rightarrow \{1, 2\}$ from user set index to serving tier index. Thus, from (2), $J(1) = 1$, $J(B) = J(\bar{B}) = 2$.

The biased received power based association model described above leads to the formation of association/coverage areas in the Euclidean plane as described below.

Definition 1. Association Region: The region of the Euclidean plane in which all users are served by an AP is called its association region. Mathematically, the association region of an AP of tier j located at x is

$$\mathcal{C}_{x_j} = \left\{ y \in \mathbb{R}^2 : \|y - x\| \leq \left(\frac{P_j B_j}{P_k B_k} \right)^{1/\alpha_j} \|y - X_k^*(y)\|^{\hat{\alpha}_k} \forall k \right\}, \quad (3)$$

where $X_k^*(y) = \arg \min_{x \in \Phi_k} \|y - x\|$.

The random tessellation formed by the collection $\{\mathcal{C}_{x_j}\}$ of

association regions is a general case of the multiplicatively weighted Voronoi [27, Chapter 3], which results by using the presented model with equal path loss exponents.

B. Resource Partitioning

A resource partitioning approach is considered in which the macro cell shuts its transmission on certain fraction of time/frequency resources and the small cell schedules the range expanded users on the corresponding resources, which protects them from macro cell interference.

Definition 2. η : The resource partitioning fraction η is the fraction of resources on which the macro cell is inactive, where $0 < \eta < 1$.

Thus, with resource partitioning $1 - \eta$ fraction of the resources at macro cell are allocated to users in \mathcal{U}_1 and those at small cell are allocated to users in $\mathcal{U}_{\bar{B}}$. The fraction η of the resources in which the macro cell shuts down the transmission, the small cells schedule the range expanded users, i.e., \mathcal{U}_B . Let γ_l denote the inverse of the effective fraction of resources available for users in \mathcal{U}_l . Then, $\gamma_l = 1/(1 - \eta)$ for $l \in \{1, \bar{B}\}$ and $\gamma_l = 1/\eta$ for $l = B$. The operation of range expansion and resource partitioning in a two-tier setup is further elucidated in Fig. 1. In these plots, the power ratio is assumed to be $\frac{P_1}{P_2} = 20$ dB and $B = 10$ dB.

As a result of resource partitioning ($0 < \eta < 1$), the SINR of a typical user u , when it belongs to \mathcal{U}_l , is

$$\text{SINR} = \mathbf{1}(l \in \{1, \bar{B}\}) \frac{P_{J(l)} H_y y^{-\alpha_{J(l)}}}{\sum_{k=1}^2 I_{y,k} + \sigma^2} + \mathbf{1}(l = B) \frac{P_2 H_y y^{-\alpha_2}}{I_{y,2} + \sigma^2}, \quad (4)$$

where $\mathbf{1}(A)$ denotes the indicator of the event A , H_y is the channel power gain from the tagged AP s_l (AP serving the typical user) at a distance y , $I_{y,k}$ denotes the interference from the k^{th} tier. The interference power from k^{th} tier is

$$I_{y,k} = P_k \sum_{x \in \Phi_k \setminus s_l} H_x x^{-\alpha_k}. \quad (5)$$

In this paper, all APs of a tier are assumed to be active, when the corresponding tier is active. However, if each AP of k^{th} tier is independently active with a probability p_{ak} , the submission in (5) can then be treated as that over a thinned PPP of density $\lambda_k p_{ak}$.

Let \mathcal{U}_s denote the set of users associated with the tagged AP. If the tagged AP belongs to macro tier, then $N_1 = |\mathcal{U}_s \cap \mathcal{U}_1|$ denotes the total number of users (or *load* henceforth) sharing the available $1 - \eta$ fraction of the resources. Otherwise, if the tagged AP belongs to tier 2, then the load is $N_2 = |\mathcal{U}_s \cap \mathcal{U}_2|$ of which $N_{\bar{B}} = |\mathcal{U}_s \cap \mathcal{U}_{\bar{B}}|$ users share the $1 - \eta$ fraction of the resources and $N_B = |\mathcal{U}_s \cap \mathcal{U}_B|$ users share the rest η ; $N_2 = N_{\bar{B}} + N_B - 1$ (one is subtracted to account for double counting of the typical user). The available resources at an AP are assumed to be shared equally among the associated users. This results in each user having a rate proportional to its link's spectral efficiency. Round-robin scheduling is an approach which results in such equipartition of resources. Further, user queues are assumed *saturated* implying that each AP always

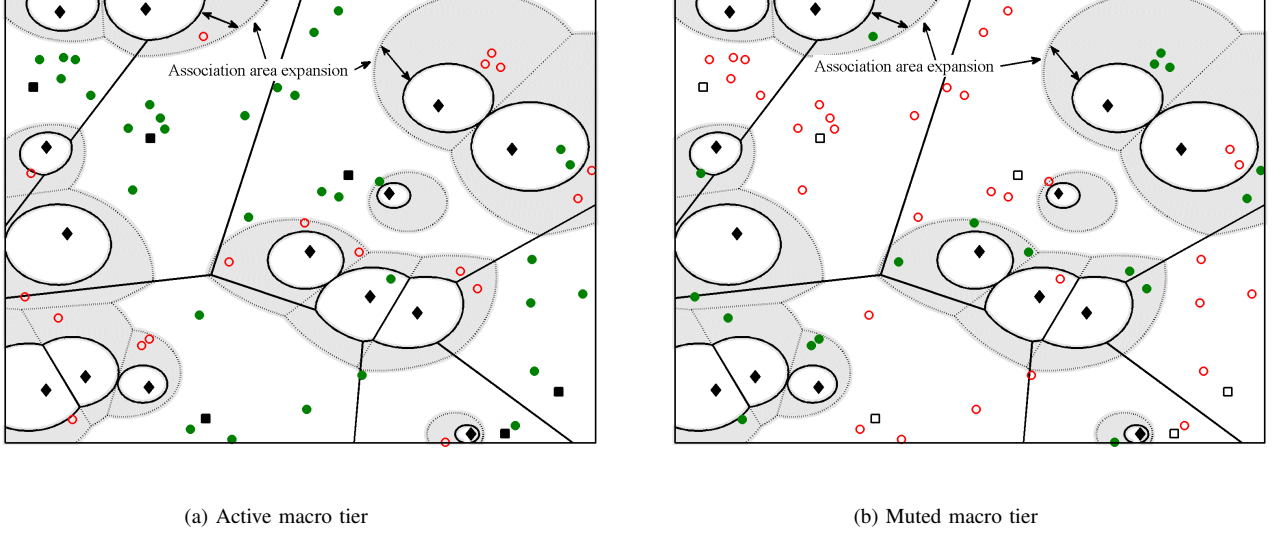


Fig. 1: A filled marker is used for a node engaged in active transmission (BS) or reception (user). (a) The macro cells (filled squares) serve the macro users \mathcal{U}_1 and small cells (filled diamonds) serve the non-range expanded users ($\mathcal{U}_{\bar{B}}$) (filled circles). (b) The macro cells (hollow square) are muted while the small cells (filled diamonds) serve the range expanded users \mathcal{U}_B (filled circles in the shaded region).

has data to transmit to its associated mobile users. Thus, the rate of a typical user u is

$$R = \sum_{l \in \{1, \bar{B}, B\}} \frac{\mathbf{1}(u \in \mathcal{U}_l)}{\gamma_l N_l} W \log(1 + \text{SINR}). \quad (6)$$

The above rate allocation model assumes infinite backhaul bandwidth for all APs, which may be particularly questionable for small cells. Discussion about limited backhaul bandwidth is deferred to Sec. III-C.

C. Rate and SINR Coverage

The rate and SINR coverage can be formally defined as follows.

Definition 3. Rate/SINR Coverage: The rate coverage for a rate threshold ρ is

$$\mathcal{R}(\rho) \triangleq \mathbb{P}(R > \rho), \quad (7)$$

and SINR coverage for a threshold τ is

$$\mathcal{S}(\tau) \triangleq \mathbb{P}(\text{SINR} > \tau). \quad (8)$$

The coverage can be equivalently interpreted as (i) the probability that a randomly chosen user can achieve a target threshold, (ii) the average fraction of users in the network who at any time achieve the corresponding threshold, or (iii) the average fraction of the network area that is receiving rate/SINR greater than the rate/SINR threshold.

III. RATE DISTRIBUTION

This section derives the load distribution and SINR distribution, which are subsequently used for deriving the rate distribution (coverage) and is the main technical section of the paper.

A. SINR Distribution

For completely characterizing the SINR and rate distribution, the average fraction of users belonging to the respective three disjoint sets (\mathcal{U}_1 , $\mathcal{U}_{\bar{B}}$, and \mathcal{U}_B) is needed. Using the ergodicity of the PPP, these fractions are equal to the association probability of a typical user to these sets, which are derived in the following lemma.

Lemma 1. (Association probabilities) The association probability, defined as $\mathcal{A}_l \triangleq \mathbb{P}(u \in \mathcal{U}_l)$, is given below for each set

$$\mathcal{A}_1 = 2\pi\lambda_1 \int_0^\infty z \exp\left(-\pi \sum_{k=1}^2 \lambda_k (\hat{P}_k \hat{B}_k)^{2/\alpha_k} z^{2/\hat{\alpha}_k}\right) dz, \quad (9)$$

$$\mathcal{A}_{\bar{B}} = 2\pi\lambda_2 \int_0^\infty z \exp\left(-\pi \sum_{k=1}^2 \lambda_k (\hat{P}_k)^{2/\alpha_k} z^{2/\hat{\alpha}_k}\right) dz, \quad (10)$$

$$\mathcal{A}_B = 2\pi\lambda_2 \int_0^\infty z \left\{ \exp\left(-\pi \sum_{k=1}^2 \lambda_k (\hat{P}_k \hat{B}_k)^{2/\alpha_k} z^{2/\hat{\alpha}_k}\right) - \exp\left(-\pi \sum_{k=1}^2 \lambda_k (\hat{P}_k)^{2/\alpha_k} z^{2/\hat{\alpha}_k}\right) \right\} dz. \quad (11)$$

If path loss exponents are same, i.e., $\alpha_k \equiv \alpha$, the association probabilities simplify to:

$$\mathcal{A}_1 = \frac{\lambda_1}{\sum_{k=1}^2 \lambda_k (\hat{P}_k \hat{B}_k)^{2/\alpha}}, \quad \mathcal{A}_{\bar{B}} = \frac{\lambda_2}{\sum_{k=1}^2 \lambda_k (\hat{P}_k)^{2/\alpha}},$$

$$\mathcal{A}_B = \frac{\lambda_2}{\sum_{k=1}^2 \lambda_k (\hat{P}_k \hat{B}_k)^{2/\alpha}} - \frac{\lambda_2}{\sum_{k=1}^2 \lambda_k (\hat{P}_k)^{2/\alpha}}. \quad (12)$$

Proof: See Appendix A. ■

Equation (12) corroborates the intuition that increasing association bias B leads to decrease in the mean population of

$$\mathcal{S}_1(\tau) = 2\pi \frac{\lambda_1}{\mathcal{A}_1} \int_0^\infty y \exp \left\{ -\frac{\tau}{\text{SNR}_1(y)} - \pi \sum_{k=1}^2 \lambda_k \hat{P}_k^{2/\alpha_k} Q(\tau, \alpha_k, \hat{B}_k) y^{2/\hat{\alpha}_k} \right\} dy \quad (14)$$

$$\mathcal{S}_{\bar{B}}(\tau) = 2\pi \frac{\lambda_2}{\mathcal{A}_{\bar{B}}} \int_0^\infty y \exp \left\{ -\frac{\tau}{\text{SNR}_2(y)} - \pi \sum_{k=1}^2 \lambda_k \hat{P}_k^{2/\alpha_k} Q(\tau, \alpha_k, 1) y^{2/\hat{\alpha}_k} \right\} dy \quad (15)$$

$$\mathcal{S}_B(\tau) = 2\pi \frac{\lambda_2}{\mathcal{A}_B} \int_0^\infty y \exp \left\{ -\frac{\tau}{\text{SNR}_2(y)} - \pi \lambda_2 Q(\tau, \alpha_2, 1) y^2 - \pi \lambda_1 \hat{P}_1^{2/\alpha_1} y^{2/\hat{\alpha}_1} \right\} \left\{ \exp \left(-\pi \lambda_1 \hat{P}_1^{2/\alpha_1} y^{2/\hat{\alpha}_1} (\hat{B}_1^{2/\alpha_1} - 1) \right) - 1 \right\} dy, \quad (16)$$

$$\mathcal{R}_1(\rho) = 2\pi \frac{\lambda_1}{\mathcal{A}_1} \sum_{n \geq 1} p_1(n) \int_0^\infty y \exp \left\{ -\frac{t(n\hat{\rho}\gamma_1)}{\text{SNR}_1(y)} - \pi \sum_{k=1}^2 \lambda_k \hat{P}_k^{2/\alpha_k} Q(t(n\hat{\rho}\gamma_1), \alpha_k, \hat{B}_k) y^{2/\hat{\alpha}_k} \right\} dy \quad (19)$$

$$\mathcal{R}_{\bar{B}}(\rho) = 2\pi \frac{\lambda_2}{\mathcal{A}_{\bar{B}}} \sum_{n \geq 1} p_{\bar{B}}(n) \int_0^\infty y \exp \left\{ -\frac{t(n\hat{\rho}\gamma_{\bar{B}})}{\text{SNR}_2(y)} - \pi \sum_{k=1}^2 \lambda_k \hat{P}_k^{2/\alpha_k} Q(t(n\hat{\rho}\gamma_{\bar{B}}), \alpha_k, 1) y^{2/\hat{\alpha}_k} \right\} dy \quad (20)$$

$$\begin{aligned} \mathcal{R}_B(\rho) = & 2\pi \frac{\lambda_2}{\mathcal{A}_B} \sum_{n \geq 1} p_B(n) \int_0^\infty y \left\{ \exp \left(-\frac{t(n\hat{\rho}\gamma_B)}{\text{SNR}_2(y)} - \pi \lambda_2 y^2 Q(t(n\hat{\rho}\gamma_B), \alpha_2, 1) - \pi \lambda_1 y^{2/\hat{\alpha}_1} (\hat{P}_1 \hat{B}_1)^{2/\alpha_1} \right) \right. \\ & \left. - \exp \left(-\frac{t(n\hat{\rho}\gamma_B)}{\text{SNR}_2(y)} - \pi \lambda_2 y^2 Q(t(n\hat{\rho}\gamma_B), \alpha_2, 1) - \pi \lambda_1 y^{2/\hat{\alpha}_1} (\hat{P}_1)^{2/\alpha_1} \right) \right\} dy, \end{aligned} \quad (21)$$

macro cell users implied by the decreasing \mathcal{A}_1 . On the other hand, the mean population of range expanded users increases implied by the increasing \mathcal{A}_B . Further, $\mathcal{A}_2 \triangleq \mathcal{A}_{\bar{B}} + \mathcal{A}_B$ is the probability of a typical user associating with the tier 2.

The conditional SINR coverage, when a typical user $u \in \mathcal{U}_l$ is $\mathcal{S}_l(\tau) \triangleq \mathbb{P}(\text{SINR} > \tau | u \in \mathcal{U}_l)$.

Lemma 2. (SINR Coverage) *For a typical user in the setup of Sec. II, the SINR coverage is*

$$\mathcal{S}(\tau) = \mathcal{A}_1 \mathcal{S}_1(\tau) + \mathcal{A}_{\bar{B}} \mathcal{S}_{\bar{B}}(\tau) + \mathcal{A}_B \mathcal{S}_B(\tau), \quad (13)$$

where the conditional SINR coverage are given by (14)-(16),

$$Q(a, b, c) = c^{2/b} + a^{2/b} \int_{(\frac{c}{a})^{2/b}}^\infty \frac{du}{1+u^{b/2}}, \text{ and } \text{SNR}_k(y) = \frac{P_k y^{-\alpha_k}}{\sigma^2}.$$

Proof: See Appendix C. ■

The result in Lemma 2 is for the most general case and involves a single numerical integration along with a lookup table for Q . The expressions can be further simplified as in the following corollary.

Corollary 1. *With noise ignored, $\text{SNR}_k \rightarrow \infty$, assuming equal path loss exponents $\alpha_k \equiv \alpha$, the SINR coverage of a typical user is*

$$\begin{aligned} \mathcal{S}(\tau) = & \frac{\lambda_1}{\sum_{k=1}^2 \lambda_k (P_k/P_1)^{2/\alpha} Q(\tau, \alpha, B_k)} \\ & + \frac{\lambda_2}{\sum_{k=1}^2 \lambda_k (P_k/P_2)^{2/\alpha} Q(\tau, \alpha, 1)} \\ & + \frac{\lambda_2}{\lambda_2 Q(\tau, \alpha, 1) + \lambda_1 \{P_1/(P_2 B_2)\}^{2/\alpha}} \\ & - \frac{\lambda_2}{\lambda_2 Q(\tau, \alpha, 1) + \lambda_1 (P_1/P_2)^{2/\alpha}}. \end{aligned} \quad (17)$$

As evident from the above Lemma and Corollary, SINR coverage is independent of the resource partitioning fraction η because of the independence of SINR on the amount of resources allocated to a user in our model. Further, the SINR distribution of the small cell users, $\mathcal{S}_{\bar{B}}$, is independent of association bias, as $\mathcal{U}_{\bar{B}}$ is independent of bias. Further insights about SINR coverage are deferred until the next section. In general, we show that SINR coverage with and without resource partitioning show considerably different behavior, which is also reflected in the rate coverage trends.

B. Main Result

Similar to the conditional SINR coverage, conditional rate coverage, when a typical user $u \in \mathcal{U}_l$ is $\mathcal{R}_l(\rho) \triangleq \mathbb{P}(R > \rho | u \in \mathcal{U}_l)$. The following theorem gives the rate distribution over the entire network.

Theorem 1. (Rate Coverage) *For a typical user in the setup of Sec. II, the rate coverage is*

$$\mathcal{R}(\rho) = \mathcal{A}_1 \mathcal{R}_1(\rho) + \mathcal{A}_{\bar{B}} \mathcal{R}_{\bar{B}}(\rho) + \mathcal{A}_B \mathcal{R}_B(\rho), \quad (18)$$

where the conditional rate coverage are given by (19)-(21), $p_l(n) \triangleq \mathbb{P}(N_l = n)$, $t(x) = 2^x - 1$, and $\hat{\rho} = \rho/W$.

Proof: Using (4) and (6), the probability that the rate requirement of a random user u is met is

$$\mathbb{P}(R > \rho) = \sum_{l \in \{1, \bar{B}, B\}} \mathbb{P}(u \in \mathcal{U}_l) \mathbb{P} \left(\frac{W}{\gamma_l N_l} \log(1 + \text{SINR}) > \rho | u \in \mathcal{U}_l \right) \quad (22)$$

$$= \sum_{l \in \{1, \bar{B}, B\}} \mathcal{A}_l \mathbb{E}_{N_l} [\mathcal{S}_l(t(\hat{\rho} N_l \gamma_l))], \quad (23)$$

$$\bar{\mathcal{R}}_1(\rho) = 2\pi \frac{\lambda_1}{\mathcal{A}_1} \int_0^\infty y \exp \left\{ -\frac{t(\hat{\rho}\bar{N}_1\gamma_1)}{\text{SNR}_1(y)} - \pi \sum_{k=1}^2 \lambda_k \hat{P}_k^{2/\alpha_k} Q(t(\hat{\rho}\bar{N}_1\gamma_1), \alpha_k, \hat{B}_k) y^{2/\hat{\alpha}_k} \right\} dy \quad (29)$$

$$\bar{\mathcal{R}}_{\bar{B}}(\rho) = 2\pi \frac{\lambda_2}{\mathcal{A}_{\bar{B}}} \int_0^\infty y \exp \left\{ -\frac{t(\hat{\rho}\bar{N}_{\bar{B}}\gamma_{\bar{B}})}{\text{SNR}_2(y)} - \pi \sum_{k=1}^2 \lambda_k \hat{P}_k^{2/\alpha_k} Q(t(\hat{\rho}\bar{N}_{\bar{B}}\gamma_{\bar{B}}), \alpha_k, 1) y^{2/\hat{\alpha}_k} \right\} dy \quad (30)$$

$$\bar{\mathcal{R}}_B(\rho) = 2\pi \frac{\lambda_2}{\mathcal{A}_B} \int_0^\infty y \exp \left\{ -\frac{t(\hat{\rho}\bar{N}_B\gamma_B)}{\text{SNR}_2(y)} - \pi \lambda_2 y^2 Q(t(\hat{\rho}\bar{N}_B\gamma_B), \alpha_2, 1) - \pi \lambda_1 y^{2/\hat{\alpha}_1} \hat{P}_1^{2/\alpha_1} \right\} \left\{ \exp \left\{ -\pi \lambda_1 \hat{P}_1^{2/\alpha_1} y^{2/\hat{\alpha}_1} (\hat{B}_1^{2/\alpha_1} - 1) \right\} - 1 \right\} dy, \quad (31)$$

where $\hat{\rho} = \rho/W$ and $t(x) = 2^x - 1$. In general, the load and SINR are correlated, as APs with larger association regions have higher load and larger user to AP distance (and hence lower SINR). However for tractability of the analysis, this dependence is ignored, as in [24], resulting in $\mathbb{E}_{N_l} [\mathcal{S}_l(t(xN_l))] = \sum_{n \geq 1} p_l(n) \mathcal{S}_l(t(xn))$, where $p_l(n) = \mathbb{P}(N_l = n)$. Using Lemma 2, the rate coverage expression is then obtained. ■

The probability mass function of the load depends on the association area, which needs to be characterized.

Remark 1. (Mean Association Area) Association area of an AP is the area of the corresponding association region. Using the ergodicity of the PPP, the mean of the association area C_k of a typical AP of k^{th} tier is $\mathbb{E}[C_k] = \frac{\mathcal{A}_k}{\lambda_k}$.

The association region of a tier 2 AP can be further partitioned into two regions. The non-shaded region in Fig. 1 surrounding a small cell at x can be characterized as

$$\mathcal{C}_{x_{\bar{B}}} \triangleq \{y \in \mathbb{R}^2 : \|y-x\| \leq (P_2/P_1)^{1/\alpha_2} \|y-X_k^*(y)\|^{\hat{\alpha}_1}, \forall k\}. \quad (24)$$

As per (2), all the users lying in $\mathcal{C}_{x_{\bar{B}}}$ are the small cell users (belonging to $\mathcal{U}_{\bar{B}}$) and recalling (3) all users lying in $\mathcal{C}_{x_B} \triangleq \mathcal{C}_{x_2} - \mathcal{C}_{x_{\bar{B}}}$ are the offloaded users that belong to \mathcal{U}_B . In Fig. 1, \mathcal{C}_{x_B} is the shaded region surrounding a tier 2 AP.

Remark 2. (Association Area Distribution) A linear scaling based approximation for the distribution of association areas proposed in [24], which matched the first moment, is generalized in this paper to the setting of resource partitioning as below

$$C_1 = C \left(\frac{\lambda_1}{\mathcal{A}_1} \right), \quad (25)$$

$$C_{\bar{B}} = C \left(\frac{\lambda_2}{\mathcal{A}_{\bar{B}}} \right), \text{ and } C_B = C \left(\frac{\lambda_2}{\mathcal{A}_B} \right), \quad (26)$$

where $C(y)$ is the area of a typical cell of a Poisson Voronoi (PV) of density y (a scale parameter).

Using the area distribution proposed in [28] for PV $C(y)$, the following lemma characterizes the probability mass function (PMF) of the load seen by a typical user.

Lemma 3. (Load PMF) The PMF of the load at tagged AP

of a typical user $u \in \mathcal{U}_l$ is

$$\begin{aligned} p_l(n) &\triangleq \mathbb{P}(N_l = n) \\ &= \frac{3.5^{3.5}}{(n-1)!} \frac{\Gamma(n+3.5)}{\Gamma(3.5)} \left(\frac{\lambda_u \mathcal{A}_l}{\lambda_{J(l)}} \right)^{n-1} \left(3.5 + \frac{\lambda_u \mathcal{A}_l}{\lambda_{J(l)}} \right)^{-(n+3.5)} \\ &\quad n \geq 1, \end{aligned} \quad (27)$$

where $\Gamma(x) = \int_0^\infty \exp(-t)t^{x-1}dt$ is the gamma function.

Proof: See Appendix B. ■

The rate distribution expression for the most general setting requires a single numerical integral after use of lookup tables for Q and Γ . The summation over n in Theorem 1 can be accurately approximated as a finite summation to a sufficiently large value, n_{\max} (say), since both the terms $p_l(n)$ and $\mathcal{S}_l(t(xn))$ decay rapidly for large n .

The rate coverage expression can be further simplified if the load at each AP is assumed to equal its mean.

Corollary 2. (Mean Load Approximation) Rate coverage with the mean load approximation is given by

$$\bar{\mathcal{R}}(\rho) = \mathcal{A}_1 \bar{\mathcal{R}}_1(\rho) + \mathcal{A}_{\bar{B}} \bar{\mathcal{R}}_{\bar{B}}(\rho) + \mathcal{A}_B \bar{\mathcal{R}}_B(\rho), \quad (28)$$

where the conditional rate coverage are given by (29)-(31) and $\bar{N}_l = \mathbb{E}[N_l] = 1 + \frac{1.28\lambda_u \mathcal{A}_l}{\lambda_{J(l)}}$.

Proof: Lemma 3 gives the first moment of load as $\mathbb{E}[N_l] = 1 + \frac{\lambda_u \mathcal{A}_l}{\lambda_{J(l)}} \mathbb{E}[C^2(1)]$. Further, using the result that $\mathbb{E}[C^2(1)] = 1.28$ [29], along with an approximation $\mathbb{E}_{N_k} [\mathcal{S}_k(t(xN_k))] \approx \mathcal{S}_k(t(x\mathbb{E}[N_k]))$, the simplified rate coverage expression is obtained. ■

The mean load approximation above simplifies the rate coverage expression by eliminating the summation over n . The numerical integral can also be eliminated by ignoring noise and assuming equal path loss exponents (as is done in Sec IV-B). As can be observed from Theorem 1 and Corollary 2, the rate coverage for range expanded users \mathcal{R}_B increases with increase in resource partitioning fraction η , as users in \mathcal{U}_B can be scheduled on a larger fraction of (macro) interference free resources. On the other hand, the rate coverage for the macro users \mathcal{R}_1 and small cell (non-range expanded) users $\mathcal{R}_{\bar{B}}$ decreases with the corresponding increase. Further insights on the effect of biasing are delegated to the next section.

C. Rate Coverage with Limited Backhaul Capacities

Analysis in the previous sections assumed infinite backhaul capacities and thus the air interface was the only bottleneck

$$\mathcal{S}_{\bar{B}j}(\tau) = 2\pi \frac{\lambda_2}{\mathcal{A}_{\bar{B}j}} \int_0^\infty y \exp \left\{ -\frac{\tau}{\text{SNR}_j(y)} - \pi \left(\sum_{k \neq j} \lambda_k \hat{P}_k^{2/\alpha_k} Q(\tau, \alpha_k, B_k) y^{2/\hat{\alpha}_k} + \lambda_j Q(\tau, \alpha_j, 1) y^2 \right) \right\} dy \quad (38)$$

$$\begin{aligned} \mathcal{S}_{Bj}(\tau) &= 2\pi \frac{\lambda_2}{\mathcal{A}_{Bj}} \int_0^\infty y \exp \left\{ -\frac{\tau}{\text{SNR}_j(y)} - \pi \left(\sum_{k \geq 2} \lambda_k \hat{P}_k^{2/\alpha_k} Q(\tau, \alpha_k, \hat{B}_k) y^{2/\hat{\alpha}_k} - \lambda_1 (\hat{P}_1 \hat{B}_1)^{2/\alpha_1} y^{2/\hat{\alpha}_1} \right) \right\} \\ &\times \prod_{k \neq j} \left\{ 1 - \exp \left(-\pi \lambda_k (\hat{P}_k \hat{B}_k)^{2/\alpha_k} y^{2/\hat{\alpha}_k} (B_j^{2/\alpha_k} - 1) \right) \right\} dy, \end{aligned} \quad (39)$$

affecting downlink rate. However, with limited backhaul capacities O_k for BSs of tier k , the rate is given by

$$R' = \mathbf{1}(u \in \mathcal{U}_1) \min \left(R, \frac{O_1}{N_1} \right) + \mathbf{1}(u \in \mathcal{U}_2) \min \left(R, \frac{O_2}{N_2} \right), \quad (32)$$

where R is the rate of the user with infinite backhaul bandwidth. The above rate allocation assumes that the available backhaul bandwidth for a BS of tier k , O_k , is shared equally among the associated users/load N_k . This allocation model is similar to the fair round robin scheduling and results in the peak rate of a typical user (associated with an AP of tier k) being capped at $\frac{O_k}{N_k}$. The analysis can be extended to incorporate a generic peak rate dependency $f(O_k, N_k)$ on backhaul bandwidth and load at the AP (which may result from a different backhaul allocation strategy)⁴. The following lemma gives the rate distribution in this setting.

Lemma 4. (Rate Coverage with Limited Backhaul) The rate coverage in the setting of Sec. II and with rate model of (32) is

$$\mathcal{R}'(\rho) = \mathbb{P}(R' > \rho) = \mathcal{A}_1 \mathcal{R}'_1(\rho) + \mathcal{A}_{\bar{B}} \mathcal{R}'_{\bar{B}}(\rho) + \mathcal{A}_B \mathcal{R}'_B(\rho), \quad (33)$$

where

$$\begin{aligned} \mathcal{R}'_1(\rho) &= \sum_{n=1}^{\lceil O_1/\rho-1 \rceil} p_1(n) \mathcal{S}_1(t(\gamma_1 n \hat{\rho})), \\ \mathcal{R}'_{\bar{B}}(\rho) &= \sum_{m=0}^{\lceil O_2/\rho-2 \rceil} p_{\bar{B}}(m) \sum_{n=1}^{\lceil O_2/\rho-m-1 \rceil} p_{\bar{B}}(n) \mathcal{S}_{\bar{B}}(t(\gamma_{\bar{B}} n \hat{\rho})), \\ \mathcal{R}'_B(\rho) &= \sum_{m=0}^{\lceil O_2/\rho-2 \rceil} p_B(m) \sum_{n=1}^{\lceil O_2/\rho-m-1 \rceil} p_B(n) \mathcal{S}_B(t(\gamma_B n \hat{\rho})), \end{aligned} \quad (34)$$

and \mathcal{S}_l is given by Lemma 2.

Proof: Since the maximum rate of a user $u \in \mathcal{U}_l$ is $O_{J(l)}/N_{J(l)}$. Thus, for this user to have positive rate coverage, i.e., $\mathbb{P}(R > \rho) > 0$, a necessary condition is $N_{J(l)} \leq \lceil \frac{O_{J(l)}}{\rho} - 1 \rceil$. When this necessary condition is satisfied, the

rate coverage is equivalent to

$$\begin{aligned} \mathcal{R}'_l &= \mathbb{P}(R' > \rho) \\ &= \mathbb{P} \left(\frac{W}{\gamma_l N_l} \log(1 + \text{SINR}) > \rho \cap \left\{ N_{J(l)} < \frac{O_{J(l)}}{\rho} \right\} \right) \end{aligned} \quad (35)$$

Using $N_l = N_{J(l)}$ for $l = 1$, and independence of $N_{\bar{B}}$ and N_B the conditional rate coverage are obtained. ■

It is evident from the above Lemma that rate coverage decreases with decreasing backhaul bandwidth. Therefore, decreasing O_2 will lead to decrease in the rate of the user when it is associated to small cell and thus decreasing the optimal offloading bias (this is further explored in subsequent sections). As the backhaul bandwidth increases to infinity, Lemma 4 leads to Theorem 1, or, $\lim_{O_{J(l)} \rightarrow \infty} \mathcal{R}'_l \rightarrow \mathcal{R}_l$.

D. Extension to Multi-tier Downlink

The analysis in the previous sections discussed a two-tier setup, which can be generalized to a K -tier ($K > 2$) setting. In this setting, location of the BSs of k^{th} tier are assumed according to a PPP Φ_k of density λ_k . Further, B_k is assumed to be the association bias corresponding to tier k , where $B_1 = 0$ dB and $B_k \geq 0$ dB $\forall k > 1$. Similar to (2), a user u associated with tier j can be classified into two disjoint sets:

$$u \in \begin{cases} \mathcal{U}_{\bar{B}j} & \text{if } P_j Z_j^{-\alpha_j} > P_k B_k Z_k^{-\alpha_k} \quad \forall k \neq j \\ \mathcal{U}_{Bj} & \text{if } u \notin \mathcal{U}_{\bar{B}j} \text{ and } P_j B_j Z_j^{-\alpha_j} > P_k B_k Z_k^{-\alpha_k} \quad \forall k \neq j. \end{cases} \quad (36)$$

With resource partitioning, an AP of tier j schedules the offloaded users, \mathcal{U}_{Bj} , in η fraction of the resources, which are protected from the macro-tier interference and the non-range expanded users are scheduled on $1 - \eta$ fraction of the resources. Thus, the SINR of a user u associated with tier j is

$$\text{SINR} = \mathbf{1}(u \in \mathcal{U}_{Bj}) \frac{P_j H_y y^{-\alpha_j}}{\sum_{k=2}^K I_{y,k} + \sigma^2} + \mathbf{1}(u \in \mathcal{U}_{\bar{B}j}) \frac{P_j H_y y^{-\alpha_j}}{\sum_{k=1}^K I_{y,k} + \sigma^2}. \quad (37)$$

By using similar techniques as in a two-tier setting, the SINR coverage for this setting is given in (38)-(39). The rate is given by

$$R = \left\{ \mathbf{1}(u \in \mathcal{U}_{Bj}) \frac{\eta}{N_{Bj}} + \mathbf{1}(u \in \mathcal{U}_{\bar{B}j}) \frac{1-\eta}{N_{\bar{B}j}} \right\} W \log(1 + \text{SINR}). \quad (40)$$

The rate coverage for this setting can be derived by using (38)-(39) and a generalization of Lemma 3.

⁴Exact analysis of wired backhaul allocation among the competing TCP flows could be an area of future investigation.

E. Validation of Analysis

We verify the developed analysis, in particular Theorem 1, Corollary 2, and Lemma 4, in this section. The rate distribution is validated by sweeping over a range of rate thresholds. The rate distribution obtained through simulation and that from Theorem 1 and Corollary 2 for two values for the pair of bias and resource partitioning fraction (B, η) is shown in Fig. 2a. The respective densities used are $\lambda_1 = 1$ BS/km², $\lambda_2 = 5$ BS/km², and $\lambda_u = 100$ users/km² with $\alpha_1 = 3.5$, $\alpha_2 = 4$. The assumed transmit powers are $P_1 = 46$ dBm and $P_2 = 26$ dBm. Thermal noise power is assumed to be $\sigma^2 = -10$ dBm. The rate distribution for the case with limited backhaul obtained through simulation and that from Lemma 4 is shown in Fig. 2b. The rate distribution is shown for two different backhaul bandwidths for a bias of $B = 10$ dB and without resource partitioning. Both the plots show that the analytical results, Theorem 1 and Lemma 4, give quite accurate (close to simulation) rate distribution. Furthermore, the mean load approximation based Corollary 2 is also not that far off from the exact curves in Fig. 2a. This gives further confidence that the rate distribution obtained with mean load approximation in Corollary 2 can be used for further insights (as is done in the following sections).

IV. INSIGHTS ON OPTIMAL SINR AND RATE COVERAGE

As it was mentioned earlier the extent of resource partitioning and offloading needs to be carefully chosen for optimal performance. Although a simplified setting is considered in the following results for analytical insights, it is shown that these insights extend to more general settings through numerical results.

A. SINR Coverage: Trends and Discussion

Although rate coverage is the main metric of interest, insights obtained from SINR coverage should be useful in explaining key trends in rate coverage. As stated before, the SINR coverage with and without resource partitioning exhibits different behavior in conjunction with offloading. The following lemma presents some key trends for SINR coverage in both settings.

Corollary 3. *Ignoring thermal noise ($\sigma^2 \rightarrow 0$), assuming equal path loss exponents and equal to four ($\alpha_k \equiv 4$ ⁵), the SINR coverage without resource partitioning is*

$$\begin{aligned} S^w(\tau) = & \frac{1}{\sqrt{\tau} \tan^{-1}(\sqrt{\tau}) + 1 + a\sqrt{p}(\sqrt{\tau} \tan^{-1}(\sqrt{\tau/b}) + \sqrt{b})} \\ & + \frac{1}{\sqrt{\tau} \tan^{-1}(\sqrt{\tau}) + 1 + \frac{1}{a\sqrt{p}}(\sqrt{\tau} \tan^{-1}(\sqrt{b\tau}) + \sqrt{1/b})}, \end{aligned} \quad (41)$$

where $b = \frac{B_2}{B_1}$, $a = \frac{\lambda_2}{\lambda_1}$, and $p = \frac{P_2}{P_1}$. The SINR coverage with

resource partitioning for the corresponding setting is

$$\begin{aligned} S(\tau) = & \frac{1}{\sqrt{\tau} \tan^{-1}(\sqrt{\tau}) + 1 + a\sqrt{p}(\sqrt{\tau} \tan^{-1}(\sqrt{\tau/b}) + \sqrt{b})} \\ & + \frac{1}{\sqrt{\tau} \tan^{-1}(\sqrt{\tau}) + 1 + \frac{1}{a\sqrt{p}}(\sqrt{\tau} \tan^{-1}(\sqrt{\tau}) + 1)} \\ & + \frac{1}{\sqrt{\tau} \tan^{-1}(\sqrt{\tau}) + 1 + \frac{1}{a\sqrt{p}b}} - \frac{1}{\sqrt{\tau} \tan^{-1}(\sqrt{\tau}) + 1 + \frac{1}{a\sqrt{p}}}. \end{aligned} \quad (42)$$

Proof: Using

$$Q(\tau, 4, x) = 1 + \sqrt{\tau} \int_{\sqrt{\frac{x}{\tau}}}^{\infty} \frac{du}{1+u^2} = 1 + \sqrt{\tau} \tan^{-1}(\sqrt{\tau/x}),$$

in Corollary 1, and substituting $a = \frac{\lambda_2}{\lambda_1}$, $p = \frac{P_2}{P_1}$, and $b = \frac{B_2}{B_1}$, the expression in (42) is obtained. For the case with no resource partitioning, the expression derived in Lemma 5 of [24] can be simplified using similar techniques to give (41). ■

Moreover, in this setting the following three claims can be made:

Claim 1: Offloading with a bias ($b > 1$) leads to suboptimal SINR coverage S^w in the case of no resource partitioning and $\tau \geq 1$ (0 dB).

Claim 2: With resource partitioning, the bias b maximizing the SINR coverage S can be greater than 0 dB, the upper bound on which, however, decreases with increasing density of small cells.

Claim 3: With resource partitioning, the SINR coverage obtained by offloading all the users to small cells, i.e., $b \rightarrow \infty$, is always less than that of no biasing, i.e., $b = 1$.

Proof: See Appendix D. ■

From the above corollary, it can be noted that $S|_{b=1} = S^w|_{b=1}$, i.e., with no biasing/offloading SINR distribution with and without resource partitioning are equal as the orthogonal resource is not utilized by any user. Further, with resource partitioning the contribution to coverage from range expanded users (third term in (42)) increases with increasing bias, whereas the corresponding contribution from the macro cell users (first term in (42)) decreases with increasing bias. This is a bit counter-intuitive as one would expect with increasing bias only very good geometry users remain with macro cell. The reasoning behind this is the *fast* decrease in the fraction of such users \mathcal{A}_1 with increasing bias, which leads to an overall decrease in the coverage contribution from macro cell users. Similarly, the corresponding *fast* increase in the fraction of offloaded users \mathcal{A}_B leads to an overall increase in the their contribution to coverage. A similar trend is observed for coverage without resource partitioning in (41).

An intuitive explanation for the claims is as follows. Claim 1 states that without resource partitioning, proactively offloading a user to small cell through an association bias is suboptimal, as the user would then always be associated to an AP offering lower SINR. On the other hand, with resource partitioning certain fraction of users can be offloaded to small cells and served on the resources which are protected from macro cell interference. In this case, increasing the small cell density, however, increases the interference on the orthogonal resources

⁵ α typically varies from 3 to 4 depending on the propagation environment.

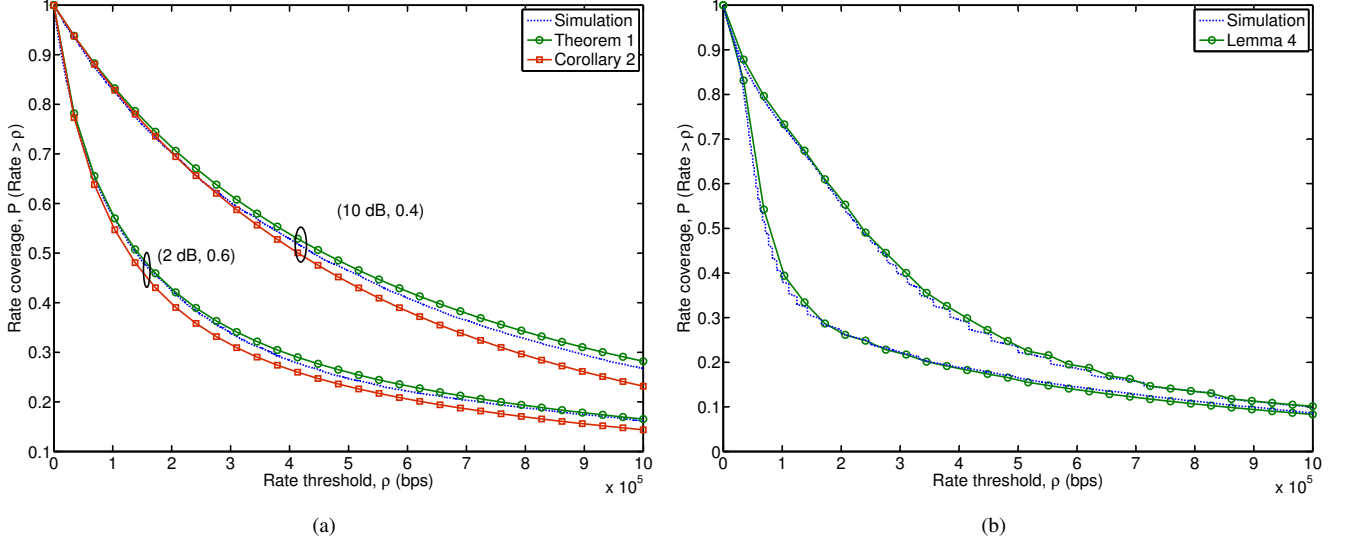


Fig. 2: (a) Rate distribution obtained from simulation, Theorem 1 and Corollary 2 for $\lambda_2 = 5\lambda_1$, $\alpha_1 = 3.5$, and $\alpha_2 = 4$. (b) Rate distribution obtained from simulation and Lemma 4 for $\lambda_2 = 5\lambda_1$, $\alpha_1 = 3.5$, and $\alpha_2 = 4$.

for the offloaded users, and hence, the optimal offloading bias is forced downward. Claim 2 justifies the described intuition when the bound is tight. Claim 3 suggests that preventing only offloaded users from macro tier interference is clearly suboptimal when almost all the macro cell users are offloaded to small cells. Of course, with large association bias, $b \rightarrow \infty$, it would be better to shut the macro tier completely off, i.e., $\eta = 1$.

The above discussion is corroborated by the results in Fig. 3, which shows the effect of association bias on SINR coverage with varying density of small cells for a setting with $\alpha_1 = 3.5$, $\alpha_2 = 4$, and $\tau = 0.5$ (-3 dB). Without resource partitioning, it can be seen that any bias is suboptimal whereas for the case with resource partitioning optimal SINR coverage decreases with increasing density and the optimal bias also decreases. In case of no resource partitioning, increase in coverage with density is observed due to higher path loss exponents of small cells (this was also observed in [19]). Thus, as evident from these results, the above claims hold in general settings too.

B. Rate Coverage: Trends and Discussion

The following Corollary provides the rate coverage expressions for a simplified setting, which is used for drawing the following insights.

Corollary 4. Ignoring thermal noise ($\sigma^2 \rightarrow 0$), assuming equal path loss exponents and equal to four ($\alpha_k \equiv 4$), the rate coverage without resource partition and with the mean load approximation is

$$\bar{\mathcal{R}}^w = \frac{1}{\sqrt{u_1} \tan^{-1}(\sqrt{u_1}) + 1 + a\sqrt{p}(\sqrt{u_1} \tan^{-1}(\sqrt{u_1/b}) + \sqrt{b})} + \frac{1}{\sqrt{u_2} \tan^{-1}(\sqrt{u_2}) + 1 + \frac{1}{a\sqrt{p}}(\tan^{-1}(\sqrt{bu_2}) + \sqrt{1/b})}. \quad (43)$$

where $u_k = t(\hat{p}\bar{N}_k)$, $b = \frac{B_2}{B_1}$, $a = \frac{\lambda_2}{\lambda_1}$, and $p = \frac{P_2}{P_1}$. The rate coverage with resource partitioning under the corresponding

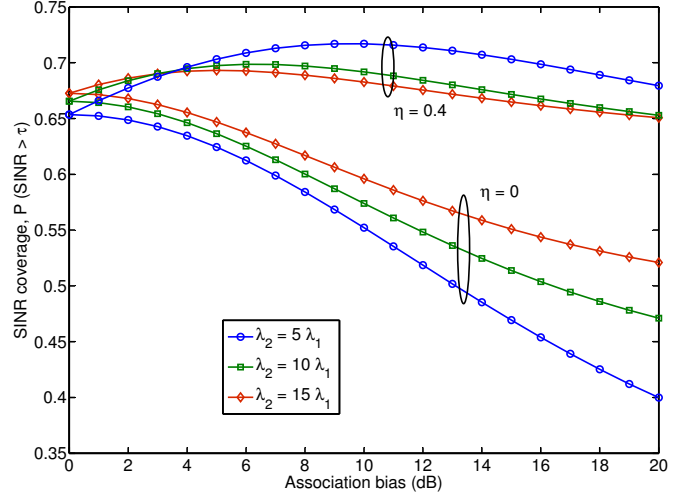


Fig. 3: Effect of small cell density on SINR coverage, with and without resource partitioning, as association bias is varied.

assumptions is

$$\bar{\mathcal{R}} = \frac{1}{\sqrt{u_1} \tan^{-1}(\sqrt{u_1}) + 1 + a\sqrt{p}(\sqrt{u_1} \tan^{-1}(\sqrt{u_1/b}) + \sqrt{b})} + \frac{1}{\sqrt{u_B} \tan^{-1}(\sqrt{u_B}) + 1 + \frac{1}{a\sqrt{p}}(\tan^{-1}(\sqrt{u_B}) + 1)} + \frac{1}{\sqrt{u_B} \tan^{-1}(\sqrt{u_B}) + 1 + \frac{1}{a\sqrt{pb}}} - \frac{1}{\sqrt{u_B} \tan^{-1}(\sqrt{u_B}) + 1 + \frac{1}{a\sqrt{p}}}, \quad (44)$$

where $u_l = t(\hat{p}\bar{N}_l\gamma_l)$.

Proof: For the case with resource partitioning, the rate coverage expression follows from Corollary 2 using similar techniques as in the proof of Corollary 3. Without any resource

partitioning Corollary 2 of [24] is used. ■

From the above expressions it can be observed that $\bar{\mathcal{R}}|_{\eta=0,b=1} = \bar{\mathcal{R}}^w|_{b=1}$, i.e., the rate distribution for both scenarios is same when no orthogonal resource is made available and there are no offloaded users. For the case with no resource partitioning, the contribution to rate coverage from macro cell users (first term of (43)) increases initially with increasing bias as the number of users sharing the radio resources at each macro BS decrease. But, beyond a certain association bias, due to the decreasing fraction of macro cell users, the overall contribution of the corresponding term towards rate coverage decreases. Similar trend is shown by the contribution from small cell users (second term in (43)). The initial increase with bias is due to the increasing fraction of small cell users and the subsequent decrease is due to increased number of users sharing the radio resources. This behavior of rate coverage could be seen as an intuitive reasoning behind the existence of an optimal bias.

With resource partitioning, decreasing η increases the rate coverage of macro cell users and small cell users (first two terms of (44) respectively), whereas that of range expanded users decreases (last two terms of (44)), due to the decrease in available radio resources. With increasing bias, the rate coverage contribution from small cell users remains invariant (second term in (44)), as the set $\mathcal{U}_{\bar{B}}$ is independent of association bias. The contribution to rate coverage from the macro cell users (first term in (44)) and that from offloaded users (sum of third and fourth term in (44)) show similar variation with association bias as in the case of no resource partitioning. Therefore, there should exist an optimal bias for each η in this setting too.

The discussion in the above paragraphs is extended further in the following sections where the impact of various factors is studied on optimal offloading. For the following results, the parameters used are the same as in Section III-E with rate threshold $\rho = 250$ Kbps wherever applicable.

1) *Impact of resource partitioning:* The effect of association bias and resource partitioning fraction on rate coverage, as obtained from Theorem 1, is shown in Fig. 4. The optimal pair for this setting is $B = 15$ dB and $\eta = 0.47$ (obtained by two-fold search), which gives a significant increase in the rate coverage compared to the case with no resource partitioning and offloading ($B = 0$ dB, $\eta = 0$). With increasing resource partitioning fraction, the optimal association bias increases as more resources (macro interference free) become available for offloaded users. The variation of rate coverage with resource partitioning fraction for different association biases is shown in Fig. 5. The optimal resource partitioning fraction increases with increase in association bias as more resources are needed to serve the increasing number of offloaded users. As shown, at lower association bias lower resource partitioning fraction is better as there are not enough range expanded users to take advantage of the resources obtained from muting the macro tier.

A trend similar to rate coverage can also be seen in the 5th percentile rate ρ_{95} (where $\mathcal{R}(\rho_{95}) = 0.95$, i.e., fifth percentile of the population receives rate less than ρ_{95}) in Fig. 6. The corresponding effect on median rate is shown

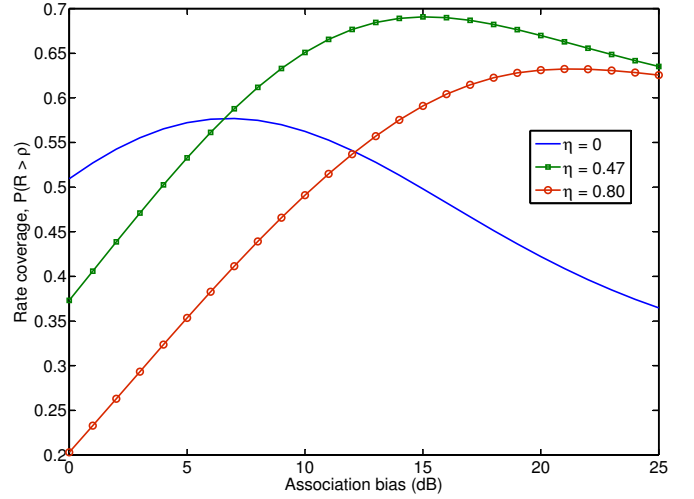


Fig. 4: Effect of association bias, B , on rate coverage with $\lambda_2 = 5\lambda_1$.

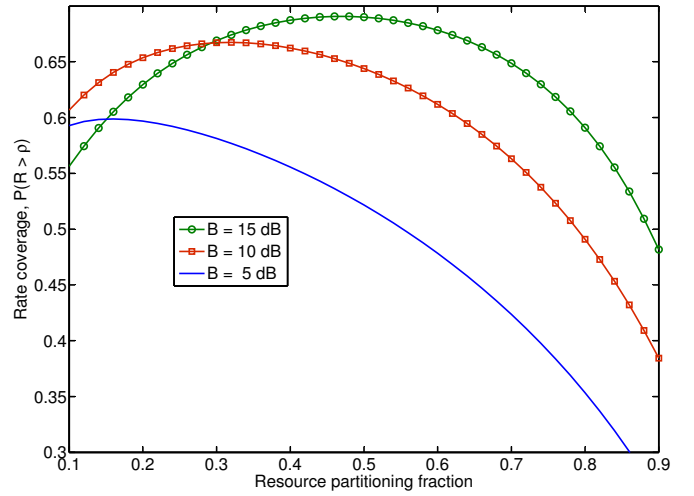


Fig. 5: Effect of resource partitioning fraction, η , on rate coverage with $\lambda_2 = 5\lambda_1$.

in Fig. 7. The optimal pair of (B, η) for these two metrics is same as that in rate coverage result. This shows that a single choice of the operating region provides a network-wide optimal performance across different metrics.

2) *Impact of infrastructure density:* The impact of density of small cells on the fifth percentile rate is shown in Fig. 8. It can be observed that at any particular association bias, as small cell density increases, ρ_{95} also increases because of the decrease in load at each AP. With no resource partitioning, $\eta = 0$, the optimal bias is seen to be invariant (at 5 dB) to the small cell density. Similar trend was also observed in [18] through exhaustive simulations. However, with resource partitioning, $\eta > 0$, optimal association bias decreases with increasing small cell density. The optimal resource partitioning fractions (also shown for each density value) decrease with increasing small cell density. These observations regarding the behavior of bias and resource partitioning fraction with small

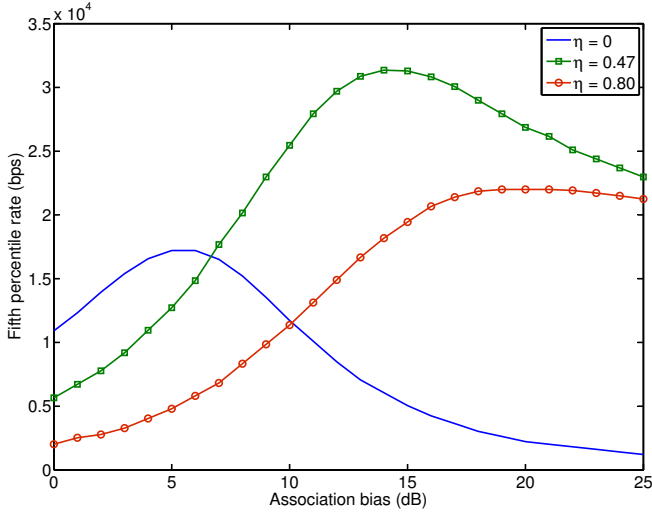


Fig. 6: Effect of association bias and resource partitioning fraction (B, η) on fifth percentile rate.

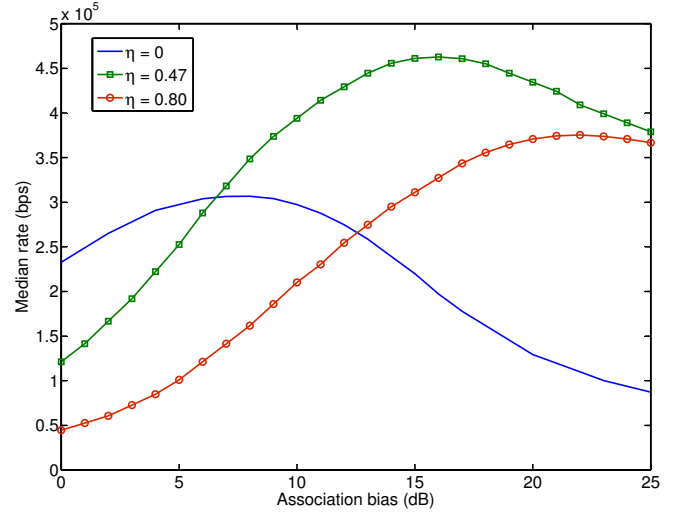


Fig. 7: Effect of association bias and resource partitioning fraction (B, η) on median rate.

cell density can be explained by re-highlighting the learning from Sec. IV-A about optimal bias for SINR coverage. Without any resource partitioning, the optimal bias for SINR coverage is 0 dB and independent of small cell density and similar independence is seen for rate coverage where the optimal bias is 5 dB. The insight of strictly suboptimal performance by a positive bias from SINR, though is clearly not valid for rate. With resource partitioning, increasing small cell density decreased the SINR coverage due to the increased interference in the orthogonal time/frequency resources allocated to range expanded users. Similar decrease of optimal association bias with increasing small cell density is seen for rate for same reasons. The increased interference in the orthogonal resources also leads to the decrease in the optimal fraction of such resources, η .

It is worth pointing here that, although, the optimal association bias decreases with increasing small cell density, the optimal traffic offload fraction \mathcal{A}_2 increases. With increasing density, at the same traffic offload fraction, the load per AP decreases, increasing the affinity of users for the corresponding tier. This trend is shown in Fig. 9 for two cases – (1) infinite backhaul bandwidth and (2) limited small cell backhaul bandwidth $O_2 = 5$ Mbps. Decreasing backhaul bandwidth lowers both the optimal bias and consequently optimal offloading fraction at a fixed density. Interestingly, with increasing density, the optimal bias for case (2) increases, in contrast to the trend in case (1). This is because of the decreasing load per AP and the, thus, diminishing performance gap between the limited and infinite backhaul setting. Therefore, beyond a certain density the gap almost vanishes and the corresponding optimal biases reduce with increasing density.

V. CONCLUSION

We have provided an analytical framework for offloading and resource partitioning in co-channel heterogeneous networks. With the heterogeneity in base stations becoming prominent in emerging wireless networks these two tech-

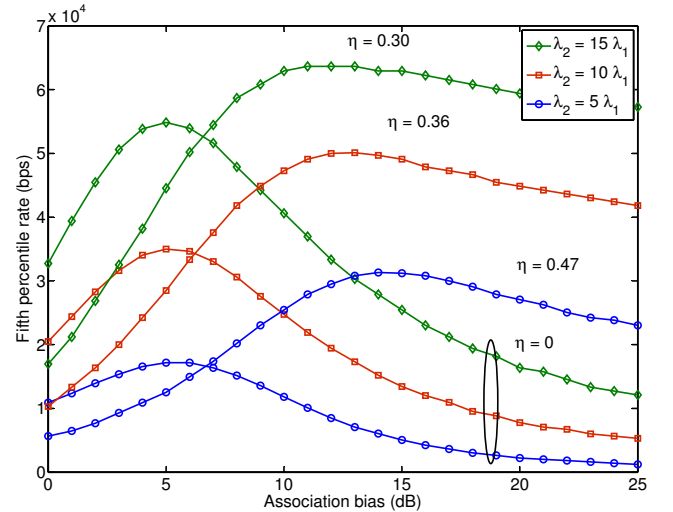


Fig. 8: Variation in fifth percentile rate with association bias and resource partitioning fraction (B, η) for different small cell densities.

niques are set to play an important role in radio resource management. To the best of our knowledge, this is first work to derive rate distribution in a heterogeneous cellular network, while incorporating resource partitioning and limited bandwidth backhauls. The availability of a functional form for rate as a function of system parameters opens a plethora of avenues to gain design insights. Using the developed analysis, the importance of combining load balancing with resource partitioning was clearly established. It was further shown that the rate is a key metric for studying these techniques and insights based on just SINR are inconclusive. Investigating the impact of offloading on rate distribution in the uplink of HetNets could be an interesting future research direction.

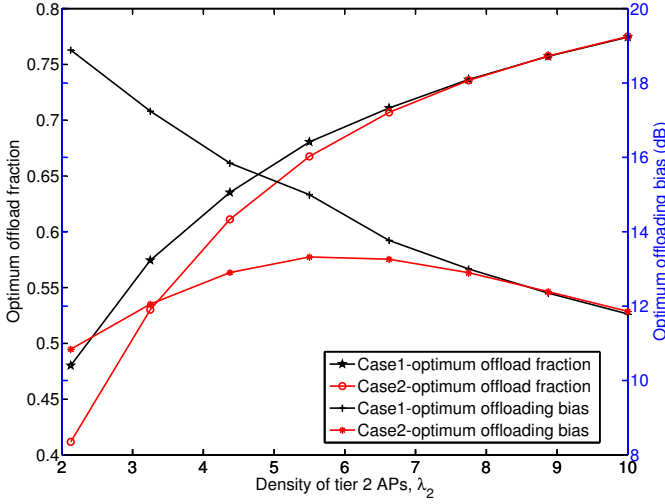


Fig. 9: Effect of backhaul bandwidth and small cell density on the optimum association bias and optimum traffic offload fraction.

APPENDIX A

Proof of Lemma 1: Using the definition of the three disjoint sets, the respective association probabilities are

$$\begin{aligned}
 \mathcal{A}_1 &= \mathbb{P} \left(P_1 Z_1^{-\alpha_1} > P_2 \hat{B}_2 Z_2^{-\alpha_2} \right) \\
 &= \int_{z>0} \mathbb{P} \left(Z_2 > (\hat{P}_2 \hat{B}_2)^{1/\alpha_2} z^{1/\hat{\alpha}_2} \right) f_{Z_1}(z) dz \\
 \mathcal{A}_{\bar{B}} &= \mathbb{P} \left(P_2 Z_2^{-\alpha_2} > P_1 Z_1^{-\alpha_1} \right) \\
 &= \int_{z>0} \mathbb{P} \left(Z_1 > (\hat{P}_1)^{1/\alpha_1} z^{1/\hat{\alpha}_1} \right) f_{Z_2}(z) dz \\
 \mathcal{A}_B &= \mathbb{P} \left(P_2 B_2 Z_2^{-\alpha_2} > P_1 Z_1^{-\alpha_1} \cap P_2 Z_2^{-\alpha_2} < P_1 Z_1^{-\alpha_1} \right) \\
 &= \int_{z>0} \mathbb{P} \left(\left(\frac{\hat{P}_1}{\hat{B}_2} \right)^{1/\alpha_1} z^{1/\hat{\alpha}_1} \leq Z_1 < (\hat{P}_1)^{1/\alpha_1} z^{1/\hat{\alpha}_1} \right) f_{Z_2}(z) dz.
 \end{aligned} \tag{45}$$

Now

$$\mathbb{P}(Z_k > z) = \mathbb{P}(\Phi_k \cap b(0, z) = \emptyset) = \exp(-\pi \lambda_k z^2), \tag{46}$$

where $b(0, z)$ is the Euclidean ball of radius z centered at origin. The probability distribution function (PDF) $f_{Z_k}(z)$ can then be written as

$$f_{Z_k}(z) = \frac{d}{dz} \{1 - \mathbb{P}(Z_k > z)\} = 2\pi \lambda_k z \exp(-\pi \lambda_k z^2), \quad \forall z \geq 0. \tag{47}$$

Using (46) and (47) in (45) gives Lemma 1. ■

APPENDIX B

Proof of Lemma 3: Assuming that the palm inversion formula [30], which relates the area of Poisson Voronoi (PV) containing the origin to that of a typical PV, holds for multiplicatively weighted PV⁶, the distribution of the

⁶Formal proof is out of the scope of this paper and will be dealt in a future publication.

association area of the tagged AP of tier- k , C'_k can be written as

$$f_{C'_k}(c) \propto c f_{C_k}(c). \tag{48}$$

For a typical user $u \in \mathcal{U}_l$, the load at the tagged AP N_l comprises of the typical user and other users $N_{o,l}$ (say) associated with the AP. Using Remark 2, the PMF of load

$$\begin{aligned}
 p_l(n) &= \mathbb{P}(N_l = n) = \int_{c>0} \exp(\lambda_u c) \frac{(\lambda_u c)^{(n-1)}}{(n-1)!} f_{C'_l}(c) dc \\
 &= \frac{3.5^{3.5}}{(n-1)!} \frac{\Gamma(n+3.5)}{\Gamma(3.5)} \left(\frac{\lambda_u \mathcal{A}_l}{\lambda_{J(l)}} \right)^{n-1} \left(3.5 + \frac{\lambda_u \mathcal{A}_l}{\lambda_{J(l)}} \right)^{-(n+3.5)} \\
 &\quad n \geq 1. \tag{49}
 \end{aligned}$$

A similar approach was taken for single-tier setting in [31] and for multi-tier setting in [24]. ■

APPENDIX C

Proof of Lemma 2: In this proof we first derive the distribution of the distance between the typical user u and the tagged AP when $u \in \mathcal{U}_l$. Let Y_l denote this distance, then

$$\mathbb{P}(Y_l > y) = \mathbb{P}(Z_{J(l)} > y | u \in \mathcal{U}_l) = \frac{\mathbb{P}(Z_{J(l)} > y, u \in \mathcal{U}_l)}{\mathbb{P}(u \in \mathcal{U}_l)}. \tag{50}$$

Using the proof of Lemma 1 in Appendix A, the corresponding PDFs are

$$\begin{aligned}
 f_{Y_1}(y) &= \frac{2\pi \lambda_1}{\mathcal{A}_1} y \exp \left(-\pi \sum_{k=1}^2 \lambda_k (\hat{P}_k \hat{B}_k)^{2/\alpha_k} y^{2/\hat{\alpha}_k} \right) \\
 f_{Y_{\bar{B}}}(y) &= \frac{2\pi \lambda_2}{\mathcal{A}_{\bar{B}}} y \exp \left(-\pi \sum_{k=1}^2 \lambda_k (\hat{P}_k)^{2/\alpha_k} y^{2/\hat{\alpha}_k} \right) \\
 f_{Y_B}(y) &= \frac{2\pi \lambda_2}{\mathcal{A}_B} y \exp \left(-\pi \sum_{k=1}^2 \lambda_k \hat{P}_k^{2/\alpha_k} y^{2/\hat{\alpha}_k} \right) \\
 &\quad \left\{ \exp \left(-\pi \sum_{k=1}^2 \lambda_k \hat{P}_k^{2/\alpha_k} y^{2/\hat{\alpha}_k} (\hat{B}_k^{2/\alpha_k} - 1) \right) - 1 \right\}.
 \end{aligned} \tag{51}$$

Conditioned on serving AP being s_l , the Laplace transform of interference can be expressed as the Laplace functional of Φ_k

$$\mathcal{L}_{I_{y,k}}(s) = \mathbb{E}_{I_{y,k}} [\exp(-s I_{y,k})] \tag{52}$$

$$= \mathbb{E} \left[\exp \left(-s P_k \sum_{x \in \Phi_k \setminus s_l} \delta_{xk} H_x x^{-\alpha_k} \right) \right] \tag{53}$$

$$\stackrel{(a)}{=} \mathbb{E}_{\Phi_k} \left[\prod_{x \in \Phi_k \setminus s_l} \mathcal{L}_{H_x}(s P_k x^{-\alpha_k}) \right] \tag{54}$$

$$\stackrel{(b)}{=} \exp \left(-2\pi \lambda_k \int_{z_{kl}(y)}^{\infty} \{1 - \mathcal{L}_{H_x}(s P_k x^{-\alpha_k})\} x dx \right) \tag{55}$$

$$\stackrel{(c)}{=} \exp \left(-2\pi \lambda_k \int_{z_{kl}(y)}^{\infty} \frac{x}{1 + (s P_k)^{-1} x^{\alpha_k}} dx \right), \tag{56}$$

where (a) follows from the independence of H_x , (b) is obtained using the PGFL [26] of Φ_k , and (c) follows by using the MGF of an exponential RV with unit mean. In the above expression, $z_{kl}(y)$ is the lower bound on distance of the closest interferer in k^{th} tier, which can be obtained by using (1) as

$$\begin{aligned} \text{if } l = 1 : z_{21}(y) &= (\hat{P}_2 \hat{B}_2)^{1/\alpha_2} y^{\alpha_1/\alpha_2}, z_{11}(y) = y \\ \text{if } l = \bar{B} : z_{1\bar{B}}(y) &= (\hat{P}_1)^{1/\alpha_2} y^{\alpha_1/\alpha_2}, z_{2\bar{B}}(y) = y \\ \text{if } l = B : z_{2B}(y) &= y \end{aligned} \quad (57)$$

Using change of variables with $t = (sP_k)^{-2/\alpha_k} x^2$, the integral can be simplified as

$$\begin{aligned} \int_{z_{kl}(y)}^{\infty} \frac{2x}{1 + (sP_k)^{-1} x^{\alpha_k}} dx &= (sP_k)^{2/\alpha_k} \int_{(sP_k)^{-2/\alpha_k} z_{kl}(y)^2}^{\infty} \frac{dt}{1 + t^{\alpha_k/2}} \\ &= (sP_k)^{2/\alpha_k} Z\left(1, \alpha_k, \frac{z_{kl}(y)^{\alpha_k}}{sP_k}\right), \end{aligned} \quad (58)$$

giving the Laplace transform of interference

$$\mathcal{L}_{I_{y,k}}(s) = \exp\left(-\pi \lambda_k (sP_k)^{2/\alpha_k} Z\left(1, \alpha_k, \frac{z_{kl}(y)^{\alpha_k}}{sP_k}\right)\right), \quad (59)$$

where

$$Z(a, b, c) = a^{2/b} \int_{(\frac{c}{a})^{2/b}}^{\infty} \frac{du}{1 + u^{b/2}}.$$

The SINR coverage of user $u \in \mathcal{U}_l$ is

$$S_l(\tau) = \int_{y \geq 0} \mathbb{P}(\text{SINR} > \tau | u \in \mathcal{U}_l, Y_l = y) f_{Y_l}(y) dy. \quad (60)$$

Using the SINR expression in (4)

$$\mathbb{P}(\text{SINR} > \tau | u \in \mathcal{U}_l, Y_l = y) = \mathbb{P}\left(\frac{P_1 H_y y^{-\alpha_1}}{\sum_{k=1}^2 I_{y,k} + \sigma^2} > \tau\right) \quad (61)$$

$$= \mathbb{P}\left(H_y > y^{\alpha_1} P_1^{-1} \tau \left\{ \sum_{k=1}^2 I_{y,k} + \sigma^2 \right\}\right) \quad (62)$$

$$= \mathbb{E}\left[\exp\left(-y^{\alpha_1} \tau P_1^{-1} \left\{ \sum_{k=1}^2 I_{y,k} + \sigma^2 \right\}\right)\right] \quad (63)$$

$$\stackrel{(a)}{=} \exp\left(-\frac{\tau}{\text{SNR}_1(y)}\right) \prod_{k=1}^2 \mathbb{E}_{I_{y,k}}\left[\exp(-y^{\alpha_1} \tau P_1^{-1} I_{y,k})\right] \quad (64)$$

$$= \exp\left(-\frac{\tau}{\text{SNR}_1(y)}\right) \prod_{k=1}^2 \mathcal{L}_{I_{y,k}}(y^{\alpha_1} \tau P_1^{-1}), \quad (65)$$

where $\text{SNR}_1(y) = \frac{P_1 y^{-\alpha_1}}{\sigma^2}$ and (a) follows from the independence of $I_{y,k}$. Similarly

$$\begin{aligned} \mathbb{P}(\text{SINR} > \tau | u \in \mathcal{U}_B, Y_l = y) \\ = \exp\left(-\frac{\tau}{\text{SNR}_2(y)}\right) \prod_{k=1}^2 \mathcal{L}_{I_{y,k}}(y^{\alpha_2} \tau P_2^{-1}), \end{aligned} \quad (66)$$

and

$$\begin{aligned} \mathbb{P}(\text{SINR}(y) > \tau | u \in \mathcal{U}_B, Y_l = y) \\ = \exp\left(-\frac{\tau}{\text{SNR}_2(y)}\right) \mathcal{L}_{I_{y,2}}(y^{\alpha_2} \tau P_2^{-1}). \end{aligned} \quad (67)$$

Using the PDF distribution (51) in (60) along with (65)-(67) and (59), the SINR coverage expressions given in Lemma 2 are obtained. The overall SINR coverage of a typical user is then obtained using the law of total probability to get $S(\tau) = \sum_l S_l(\tau) \mathcal{A}_l$. ■

APPENDIX D

Proof of claims: **Claim 1:** The partial derivative of S^w with respect to offloading bias b is

$$\begin{aligned} -a\sqrt{p} \frac{-\frac{\tau}{b+\tau} \frac{1}{2\sqrt{b}} + \frac{1}{2\sqrt{b}}}{\left\{ \sqrt{\tau} \tan^{-1}(\sqrt{\tau}) + 1 + a\sqrt{p}(\sqrt{\tau} \tan^{-1}(\sqrt{\tau/b}) + \sqrt{b}) \right\}^2} \\ - \frac{1}{a\sqrt{p}} \frac{\frac{\tau}{1+\tau b} - \frac{1}{2b^{3/2}}}{\left\{ \sqrt{\tau} \tan^{-1}(\sqrt{\tau}) + 1 + \frac{1}{a\sqrt{p}}(\sqrt{\tau} \tan^{-1}(\sqrt{b\tau}) + \sqrt{1/b}) \right\}^2}. \end{aligned}$$

Since $b, \tau \geq 0$, hence $-\frac{\tau}{b+\tau} \frac{1}{2\sqrt{b}} + \frac{1}{2\sqrt{b}} \geq 0$. Also, if

$$\tau \geq 1 \implies \tau \geq 1/b \text{ for } b \geq 1 \implies \tau \geq \frac{1}{2b^{3/2} - b} \quad (68)$$

$$\implies \frac{\tau}{1+\tau b} - \frac{1}{2b^{3/2}} \geq 0 \implies \nabla_b S^w \leq 0. \quad (69)$$

Thus, for $\tau \geq 1$ the SINR coverage decreases for all $b \geq 1$.

Claim 2: Approximating $\tan^{-1}(a) \approx a$ and substituting x for \sqrt{b} , the partial derivative of coverage with respect to x is

$$\begin{aligned} \nabla_x \mathcal{S} = \nabla_x \left\{ \frac{1}{\sqrt{\tau} \tan^{-1}(\sqrt{\tau}) + 1 + a\sqrt{p}(\frac{\tau}{x} + x)} \right. \\ \left. + \frac{1}{\sqrt{\tau} \tan^{-1}(\sqrt{\tau}) + 1 + \frac{1}{a\sqrt{px}}} \right\} \end{aligned} \quad (70)$$

$$= \frac{a\sqrt{p}(\frac{\tau}{x^2} - 1)}{\left\{ v + a\sqrt{p}(\frac{\tau}{x} + x) \right\}^2} + \frac{1}{a\sqrt{p}x^2(v + \frac{1}{a\sqrt{px}})^2}, \quad (71)$$

where $v \triangleq \sqrt{\tau} \tan^{-1}(\sqrt{\tau}) + 1$. The roots of the equation $\nabla_x \mathcal{S} = 0$ are the zeros of the polynomial

$$\begin{aligned} P(x) &= x^4 a^2 p (v^2 - 1) + 2x^3 a \sqrt{p} v (1 - \tau) \\ &- x^2 \{v^2 - 1 + a^2 p \tau (v^2 + 2)\} - 4x a \sqrt{p} v \tau - a^2 p \tau^2 - \tau. \end{aligned} \quad (72)$$

Since $v > 1$, using the Descartes sign rule the polynomial $P(x)$ has 1 positive root and upto 3 negative roots. The value of the positive root can be upper bounded [32] by

$$\begin{aligned} U = \max \left\{ \left[\frac{v^2 - 1 + a^2 p \tau (v^2 + 2)}{a^2 p (v^2 - 1)} \right]^{1/2}, \right. \\ \left. \left[\frac{4a\sqrt{p}v}{a^2 p (v^2 - 1)} \right]^{1/3}, \left[\frac{a^2 p \tau^2 + \tau}{a^2 p (v^2 - 1)} \right]^{1/4} \right\} \text{ if } \tau \leq 1 \end{aligned} \quad (73)$$

$$\begin{aligned} U = \max \left\{ \left[\frac{4a\sqrt{p}v(\tau - 1)}{a^2 p (v^2 - 1)} \right], \left[\frac{v^2 - 1 + a^2 p \tau (v^2 + 2)}{a^2 p (v^2 - 1)} \right]^{1/2}, \right. \\ \left. \left[\frac{4a\sqrt{p}v}{a^2 p (v^2 - 1)} \right]^{1/3}, \left[\frac{a^2 p \tau^2 + \tau}{a^2 p (v^2 - 1)} \right]^{1/4} \right\} \text{ if } \tau > 1. \end{aligned} \quad (74)$$

Further, the upper bound on the positive roots of $P(-x)$ is given by

$$L = \max \left\{ \left[2 \frac{v^2 - 1 + a^2 p \tau (v^2 + 2)}{a^2 p (v^2 - 1)} \right]^{1/2}, \left[2 \frac{a^2 p \tau^2 + \tau}{a^2 p (v^2 - 1)} \right]^{1/4} \right\} \text{ if } \tau > 1 \quad (75)$$

$$L = \max \left\{ \left[3 \frac{2a\sqrt{p}v(1-\tau)}{a^2 p (v^2 - 1)} \right], \left[3 \frac{v^2 - 1 + a^2 p \tau (v^2 + 2)}{a^2 p (v^2 - 1)} \right]^{1/2}, \left[3 \frac{a^2 p \tau^2 + \tau}{a^2 p (v^2 - 1)} \right]^{1/4} \right\} \text{ if } \tau \leq 1. \quad (76)$$

Note that $-L$ is the lower bound on the negative roots of $P(x)$, since they are same as the positive roots of $P(-x)$. Clearly, both U and L are inversely proportional to the density of small cells a . Since

$$-L \leq \sqrt{b} \leq U \implies b \leq \max \{U^2, L^2\}, \quad (77)$$

therefore the upper bound on optimal bias is inversely proportional to the density of small cells a .

Claim 3: The SINR coverage at very large offloading bias is

$$\mathcal{S}|_{b=\infty} \triangleq \lim_{b \rightarrow \infty} \mathcal{S} \quad (78)$$

$$= \frac{1}{v + \frac{v}{a\sqrt{p}}} + \frac{1}{v} - \frac{1}{v + \frac{1}{a\sqrt{p}}}, \quad (79)$$

where $v \triangleq \sqrt{\tau} \tan^{-1}(\sqrt{\tau}) + 1$. With the knowledge that $\mathcal{S}|_{b=1} = \mathcal{S}^w|_{b=1}$ we get

$$\mathcal{S}|_{b=1} - \mathcal{S}|_{b=\infty} = \frac{1}{v + av} - \frac{1}{v} + \frac{1}{v + \frac{1}{a}} = \frac{v^2 - v}{v(v + \frac{1}{a})(v + av)} > 0 \text{ since } v > 1.$$

Thus, $\mathcal{S}|_{b=\infty} < \mathcal{S}|_{b=1}$. ■

REFERENCES

- [1] S. Singh and J. G. Andrews, "Rate distribution in heterogeneous cellular networks with resource partitioning and offloading," in *IEEE Globecom*, Dec. 2013.
- [2] M. Alouini and A. Goldsmith, "Area spectral efficiency of cellular mobile radio systems," *IEEE Trans. Veh. Technol.*, vol. 48, pp. 1047–1066, May 1999.
- [3] A. Damnjanovic, J. Montojo, Y. Wei, T. Ji, T. Luo, M. Vajapeyam, T. Yoo, O. Song, and D. Malladi, "A survey on 3GPP heterogeneous networks," *IEEE Wireless Commun. Mag.*, vol. 18, pp. 10–21, June 2011.
- [4] A. Ghosh *et al.*, "Heterogeneous cellular networks: From theory to practice," *IEEE Commun. Mag.*, vol. 50, pp. 54–64, June 2012.
- [5] S. Singh, J. G. Andrews, and G. de Veciana, "Interference shaping for improved quality of experience for real-time video streaming," *IEEE J. Sel. Areas Commun.*, vol. 30, pp. 1259–1269, Aug. 2012.
- [6] R. Madan, J. Borran, A. Sampath, N. Bhushan, A. Khandekar, and T. Ji, "Cell association and interference coordination in heterogeneous LTE-A cellular networks," *IEEE J. Sel. Areas Commun.*, vol. 28, pp. 1479–1489, Dec. 2010.
- [7] D. Lopez-Perez, I. Guvenc, G. De La Roche, M. Kountouris, T. Quek, and J. Zhang, "Enhanced intercell interference coordination challenges in heterogeneous networks," *IEEE Wireless Commun. Mag.*, vol. 18, pp. 22–30, June 2011.
- [8] M. Vajapeyam, A. Damnjanovic, J. Montojo, T. Ji, Y. Wei, and D. Malladi, "Downlink FTP performance of heterogeneous networks for LTE-Advanced," in *IEEE ICC*, June 2011.
- [9] Y. Wang and K. Pedersen, "Performance analysis of enhanced inter-cell interference coordination in LTE-Advanced heterogeneous networks," in *IEEE VTC*, May 2012.
- [10] Nokia Siemens Networks, Nokia, "Aspects of pico node range extension," 3GPP TSG RAN WG1 meeting 61, R1-103824, 2010. Available at: <http://goo.gl/XDKXI>.
- [11] A. Barbieri, P. Gaal, S. Geirhofer, T. Ji, D. Malladi, Y. Wei, and F. Xue, "Coordinated downlink multi-point communications in heterogeneous cellular networks," in *ITA Workshop*, pp. 7–16, Feb. 2012.
- [12] Y. Wang, B. Soret, and K. Pedersen, "Sensitivity study of optimal eICIC configurations in different heterogeneous network scenarios," in *IEEE ICC*, pp. 6792–6796, June 2012.
- [13] S. Mukherjee and I. Guvenc, "Effects of range expansion and interference coordination on capacity and fairness in heterogeneous networks," in *Asilomar Conference on Signals, Systems and Computers (ASILOMAR)*, pp. 1855–1859, Nov. 2011.
- [14] T. D. Novlan, R. K. Ganti, A. Ghosh, and J. G. Andrews, "Analytical evaluation of fractional frequency reuse for heterogeneous cellular networks," *IEEE Trans. Commun.*, vol. 60, pp. 2029–2039, July 2012.
- [15] D. López-Pérez, X. Chu, and I. Guvenc, "On the expanded region of picocells in heterogeneous networks," *IEEE J. Sel. Topics Signal Process.*, vol. 6, pp. 281–294, June 2012.
- [16] M. Cierny, H. Wang, R. Wichman, Z. Ding, and C. Wijting, "On number of almost blank subframes in heterogeneous cellular networks," *IEEE Trans. Wireless Commun.*, to appear. Available at: <http://arxiv.org/abs/1304.2269>.
- [17] I. Guvenc, "Capacity and fairness analysis of heterogeneous networks with range expansion and interference coordination," *IEEE Commun. Lett.*, vol. 15, pp. 1084–1087, Oct. 2011.
- [18] Q. Ye, B. Rong, Y. Chen, M. Al-Shalash, C. Caramanis, and J. G. Andrews, "User association for load balancing in heterogeneous cellular networks," *IEEE Trans. Wireless Commun.*, vol. 12, no. 6, pp. 2706–2716, 2013.
- [19] H.-S. Jo, Y. J. Sang, P. Xia, and J. G. Andrews, "Heterogeneous cellular networks with flexible cell association: A comprehensive downlink SINR analysis," *IEEE Trans. Wireless Commun.*, vol. 11, pp. 3484–3495, Oct. 2012.
- [20] H. S. Dhillon, R. K. Ganti, F. Baccelli, and J. G. Andrews, "Modeling and analysis of K -tier downlink heterogeneous cellular networks," *IEEE J. Sel. Areas Commun.*, vol. 30, pp. 550–560, Apr. 2012.
- [21] S. Mukherjee, "Distribution of downlink SINR in heterogeneous cellular networks," *IEEE J. Sel. Areas Commun.*, vol. 30, pp. 575–585, Apr. 2012.
- [22] J. G. Andrews, F. Baccelli, and R. K. Ganti, "A tractable approach to coverage and rate in cellular networks," *IEEE Trans. Commun.*, vol. 59, pp. 3122–3134, Nov. 2011.
- [23] B. Blaszczyzyn, M. K. Karay, and H.-P. Keeler, "Using Poisson processes to model lattice cellular networks," in *Proc. IEEE INFOCOM*, pp. 773–781, Apr. 2013.
- [24] S. Singh, H. S. Dhillon, and J. G. Andrews, "Offloading in heterogeneous networks: Modeling, analysis, and design insights," *IEEE Trans. Wireless Commun.*, vol. 12, pp. 2484–2497, May 2013.
- [25] F. Baccelli, B. Blaszczyzyn, and P. Muhlethaler, "Stochastic analysis of spatial and opportunistic Aloha," *IEEE J. Sel. Areas Commun.*, pp. 1105–1119, Sept. 2009.
- [26] D. Stoyan, W. Kendall, and J. Mecke, *Stochastic Geometry and Its Applications*. John Wiley & Sons, 1996.
- [27] A. Okabe, B. Boots, K. Sugihara, and S. N. Chiu, *Spatial tessellations: Concepts and applications of Voronoi diagrams*. Probability and Statistics, NYC: Wiley, 2nd ed., 2000.
- [28] J.-S. Ferenc and Z. Nédá, "On the size distribution of Poisson Voronoi cells," *Physica A: Statistical Mechanics and its Applications*, vol. 385, pp. 518–526, Nov. 2007.
- [29] E. N. Gilbert, "Random subdivisions of space into crystals," *The Annals of Mathematical Statistics*, vol. 33, pp. 958–972, Sept. 1962.
- [30] J. Möller, *Lectures on random Voronoi tessellations*, vol. 87 of *Lecture Notes in Statistics*. New York: Springer-Verlag, 1994.
- [31] S. M. Yu and S.-L. Kim, "Downlink capacity and base station density in cellular networks," in *Workshop in Spatial Stochastic Models for Wireless Networks*, May 2013. Available at: <http://arxiv.org/abs/1109.2992>.
- [32] D. Ștefănescu, "New bounds for positive roots of polynomials," *Journal of Universal Computer Science*, vol. 11, pp. 2125–2131, Dec. 2005.